

Two new microscopical variants of thermomechanical modulation: scanning thermal expansion microscopy and dynamic localized thermomechanical analysis

A. HAMMICHE*, D. M. PRICE†, E. DUPAS‡, G. MILLS§, A. KULIK‡, M. READING†, J. M. R. WEAVER§ & H. M. POLLOCK*

*School of Physics and Chemistry, Lancaster University, Lancaster LA1 4YB, U.K.

†IPTME, Loughborough University, Loughborough LE11 3TU, U.K.

‡Swiss Federal Institute of Technology, 1015 Lausanne, Switzerland

§Department of Electronics and Electrical Engineering, University of Glasgow, Glasgow G12 8LT, U.K.

Key words. DMA, glass transition, micro-thermal analysis, scanning thermal microscopy, thermal expansion, thermomechanical modulation.

Summary

We describe two ways in which thermomechanical modulation may be used in conjunction with scanning thermal microscopy, in order to distinguish between different components of an inhomogeneous sample. The sample is subjected to a modulated mechanical stress, and the heating is supplied locally by the probe itself.

Scanning thermal expansion microscopy is an imaging mode, in which an imposed localized temperature modulation is used to generate thermal expansion, which in turn produces mechanical strain and gives thermal expansion contrast images. We present results using two types of active thermal probe. For polymer/resin samples, the depth of material contributing to the measured thermal expansion is typically a few micrometres. Under certain conditions we observe a reversal in contrast as the frequency of the temperature modulation is increased.

In dynamic localized thermomechanical analysis, the modulated stress is applied directly, and accompanied by a localized temperature change, as used in other forms of localized thermal analysis. The resulting modulated lateral force signals are obtained. The glass transition of polystyrene is detected, and shows a significant variation with frequency. The amplitude or phase signal may be used to obtain image contrast for inhomogeneous samples.

Introduction

The combination of localized thermal analysis with near-field microscopy has been termed microthermal analysis (Fryer

et al., 1998; Price *et al.*, 1998; Price *et al.*, 1999). The parent technique is that of scanning thermal microscopy, in which an 'active' thermal probe is also used as a heater, so as to allow imaging of polymers and other materials (Pollock *et al.*, 1998). The subsurface detail detected corresponds to variations in thermal conductivity or heat capacity. Localized thermal analysis (L-TA) builds upon this technique (Hammiche *et al.*, 1996a) in order to add spatial discrimination to three well-established methods of chemical fingerprinting, namely thermomechanometry, calorimetry and spectroscopy. As described in the above references, microthermal analysis has been applied to a variety of materials, including drugs (paracetamol), phase-separated polymer blends, branched polyethylenes of varying degree of crystallinity, copolymer core-shell latex films, polymer components (coatings and printed material, barrier layers, weld joints), a polymer/metal/adhesive composite, and the waxy coating on a leaf.

There are potential advantages in widening the scope of L-TA so as to include the use of mechanical modulation. Thermomechanical analysis (TMA) and dynamic mechanical analysis (DMA) are well-established techniques for characterizing a material's properties as a function of temperature (Reading & Haines, 1995). For TMA, the dimensions of a sample are measured whilst it is subjected to a constant deformation. In this way, thermal expansion coefficients can be measured and softening temperatures determined. DMA subjects the sample to an oscillating deformation so as to measure the real and imaginary parts of the elastic modulus, i.e. stiffness and damping factor (in thermal analysis, the term 'dynamic' is often used to indicate a change in mechanical force, usually in a cyclic sense). As the sample is heated, the temperature at which

Correspondence to: H. M. Pollock. Fax: + 44 (0)1524 844037; e-mail: h.pollock@lancaster.ac.uk

changes in these properties occur can be used to reveal, for example, the glass–rubber transition temperature of a polymer with very high sensitivity. Measurements are typically carried out on specimens with dimensions of several millimetres along the shortest axis, and require that slow heating rates are used so as to minimize thermal gradients within the specimen. The results of such experiments represent the sum of all of the constituents in the specimen, and the thermal response is often dominated by the higher concentration of the matrix or substrate material. It is difficult to gain detailed characterization of dilute components, contaminants and less dominant phases without physically altering the sample. In addition, TMA and DMA experiments can be very time-consuming.

In Oulevey *et al.* (2000), we describe experiments in which a sample was mounted on a vibrating heating stage; we observed the resulting amplitude and phase of the motion of an atomic force microscope cantilever, thus obtaining information on local elastic and viscoelastic properties. By contrast, the L-TA methods referenced above and described here use a miniature resistive heater–thermometer as a type of atomic force microscopy probe, and afford information equivalent to that given by TMA while measuring areas of only a few square micrometres. Not only can discrete regions of a specimen be investigated, such as individual layers in a laminated structure, but also high heating rates (of the order of 10–100 times that of conventional thermal analysis) can be employed, owing to the small size of the thermal probe and the area that it heats. These techniques differ from hot stage microscopy methods in that (a) the data are obtained from localized regions chosen from a previously obtained image, (b) apart from these regions, the rest of the sample is preserved in its original unheated state. Moreover, in principle it should be possible to develop versions of microscopy in which the image contrast is determined by spatial variations in the strength of any of these localized thermal analysis signals.

Here we describe two ways in which thermomechanical modulation may be used in this context: scanning thermal expansion microscopy (SThEM) and dynamic localized thermomechanical analysis (dynamic L-TMA). In both, the heating is localized and the sample is subjected to a modulated mechanical stress. SThEM is an imaging mode, in which an imposed localized temperature modulation is used to generate thermal expansion, which in turn produces mechanical strain. Such localized temperature modulation is already used in a.c. scanning thermal microscopy, where the subsurface detail detected corresponds to variations in heat capacity as well as in thermal conductivity; by suitably choosing the temperature modulation frequency, and hence the penetration depth of the evanescent temperature wave, we control the depth of material below the sample surface that is contributing to the image. In dynamic L-TMA, the modulated stress is

applied directly, and accompanied by a localized temperature change as used in other forms of L-TA. Some preliminary dynamic thermomechanical analysis experiments are mentioned in Reading *et al.* (1998; see Fig. 11).

Experimental

SThEM

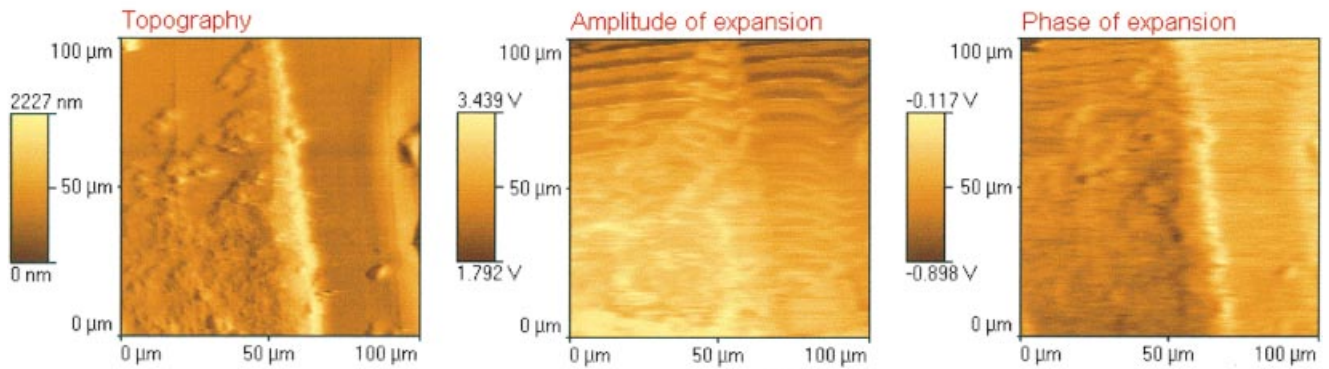
Varesi & Majumdar (1998) have described a method of thermal expansion imaging, termed scanning Joule expansion microscopy, in which Joule heating is applied by means of a modulated electric current passed through an electrically conducting sample. A conventional atomic force microscopy probe is used to detect the modulated thermal expansion for purposes of imaging. Our technique differs from this, in that we use ‘active’ thermal probes which serve as heater as well as thermometer. One type of probe (the ‘Wollaston probe’) is made from Wollaston process wire, consisting of 75 μm diameter silver wire containing a 5 μm diameter platinum/10% rhodium core, which is exposed at its end by removal of the silver. This has been widely used in micro-TA (Fryer *et al.*, 1998; Price *et al.*, 1998, 1999). The second type, termed the micromachined probe, is made at Glasgow University by photo- and electron beam lithography (Zhou *et al.*, 1998). Measurements are made using a ThermoMicroscopes (formerly TopoMetrix, Bicester, U.K.) Explorer scanning probe microscope. As shown in Fig. 1 of Hammiche *et al.* (1996b), an external source is used to apply an alternating current of chosen frequency ω_c to the probe as it is scanned across the surface at a constant underlying contact force. The a.c. current modulates the tip temperature at $\omega = 2\omega_c$. Heat transfer from the tip to the specimen results in thermal expansion of the surface at the same frequency. This causes modulated deflection of the probe height which is detected using the AFM z-axis feedback system. Its amplitude and phase shift (with regard to the heating current) are recorded using a lock-in amplifier, and the output is used to create the thermal expansion images. Appropriate values of time constants (force feedback and lock-in) and spatial scanning speed were used to minimize artefacts. Three images are recorded simultaneously: topography, amplitude of surface expansion and phase of surface expansion.

For this work we used a composite polymeric sample. A 0.5 mm thick square of polyethylene terephthalate (PET) was immersed in a resin. The resin was cured by heating at 60 °C for 24 h. The sample was then microtomed to achieve as flat a surface as possible, revealing the embedded PET.

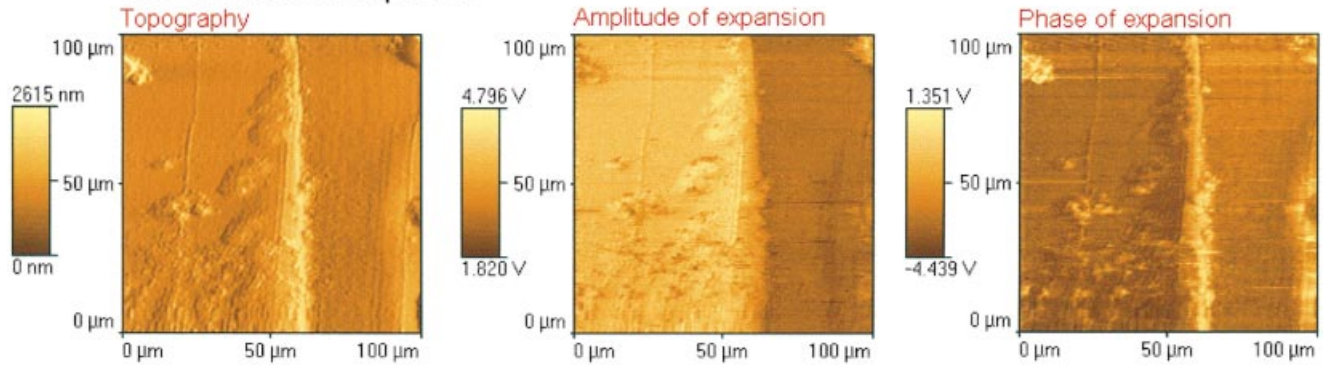
Dynamic L-TMA

Here we used a ThermoMicroscopes (Park) Autoprobe system, in which the sample, rather than the probe, is spatially scanned. As a means of applying the mechanical

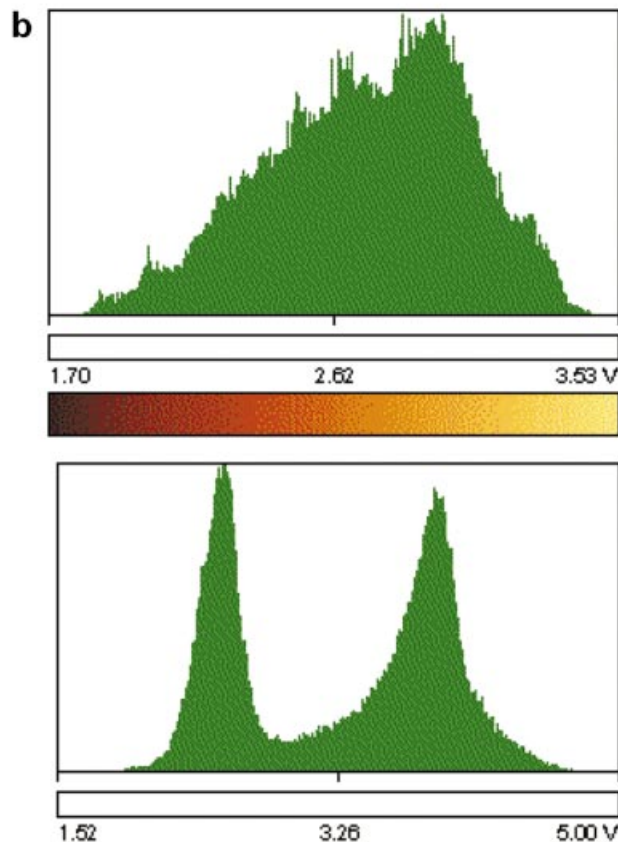
a Wollaston wire probe



Micromachined probe



resin PET



modulation, we used an isolation transformer to modulate the scanner driving voltage. The temperature ramp is applied locally, using the Wollaston thermal probe. Otherwise, the details of the set-up are as given in Oulevey *et al.* (1998), but an important feature of our current technique is that this modulation is applied to the sample in the plane of its surface (along the direction in which the probe is stiffest: this is denoted by x , and the normal direction by z). This is in contrast to our first dynamic L-TMA experiments (see Fig. 11 of Reading *et al.*, 1998), in which z -modulation was used.

We chose to use the in-plane direction of modulation in order to avoid the spurious lateral force signal that can result from friction, as shown by Mazeran & Loubet (1997) in their analysis of force modulation microscopy. They analysed the drawbacks of using z -modulation: the tilt of cantilever produces unwanted x - and y -displacement, and given the finite lateral compliance of the cantilever, the detected z -signal is generally dominated by friction. Even if the modulation amplitude is reduced to the point where no sliding occurs, this z -signal is sensitive to lateral rather than normal stiffness (unless the contact stiffness is as low as that of the cantilever). In our method, we use the instrument's lateral force facility to detect the lateral stiffness variations that result from the modulated shear strain applied. The exact orientation of the probe has a large effect on the lateral force signal; we took care to ensure (by tilting the microscope if necessary) that the probe was at 90° to the surface, as regards possible rotation in the plane of the loop ('azimuthal' angle). It is necessary also to check the alignment of the axes of the photodetector with the centre position of the light spot, as the cantilever's z -movements may give a false indication of lateral force (and vice versa).

The signals measured were as follows:

- sample scanner: z -position (d.c.) For a given cantilever stiffness, this determines the normal force (' z -force'). In general, as with other forms of localized mechanometry, force feedback was not used during data acquisition.

- lateral force (d.c., along x)
- lateral force signal along x (amplitude)
- lateral force signal along x (phase)

We find also that it is possible to obtain images whose contrast is determined by variations in these lateral signals.

The choice of frequency range is governed by the need to

keep below the resonant frequency of the system of scanner tube plus sample. This was approximately 10 kHz. For the reasons discussed above, we took care to restrict the modulation amplitude to below 10% of that needed to produce sliding. This critical value was successfully detected from observations of the lateral force signal; as the modulation amplitude was increased, a sudden onset of sliding was evident from the appearance of a hysteresis loop in the lateral force trace.

As with other types of localized thermal analysis (Hammiche *et al.*, 1996b), the required temperature change was applied by means of the heated probe placed in contact with a particular region of the sample. For this preliminary study, we used the Wollaston probe and the heating and cooling rates used were very slow, typically between 5 and 8°C min^{-1} . We used no temperature modulation. The probe temperature was calibrated by detecting the melting of four materials: polycaprolactone (56°C), low-density polyethylene (121°C), Nylon-11 (195°C) and polyethylene terephthalate (260°C) – values from conventional thermal analysis measurements on the same materials. The data presented here were all obtained in experiments on a technical polystyrene sample, whose exact molecular weight distribution is unknown. The sample was cut with a scalpel and polished with $4\ \mu\text{m}$ SiC powder, and glued onto a piezoelectric transducer with cyanolacrylate adhesive. Because this material had been injection-moulded beforehand, we annealed it *ex situ* at 110°C before gluing, in order to relax any residual internal stresses resulting from the moulding.

SThEM: results and interpretation

Thermal expansion contrast

Three types of image of the PET/resin sample were obtained: topographic, amplitude of expansion, and phase of expansion, obtained simultaneously from a given area. Modulation frequencies ranged from 30 Hz to 10 kHz. Figure 1(a) shows images obtained at 350 Hz. The amplitude of the induced probe temperature is estimated at 10°C . We see that with appropriate modulation settings, thermal expansion contrast is indeed obtained, when either the Wollaston probe or the micromachined probe is used. In general, amplitude images give more contrast than phase images, and the amplitude of the surface expansion is larger for the

Fig. 1. SThEM: modulated thermal expansion contrast. Sample: PET/resin composite. Probe temperature modulation: amplitude 10°C , frequency $\omega = 350\ \text{Hz}$. (a) Images showing cross-section of the boundary between resin (left side) and PET (right). In the amplitude and phase images, the modulated deflection of probe, detected at 2ω , determines image contrast. (b) Histograms of image contrast level (amplitude signals. Above: Wollaston probe; below, micromachined probe). The resin shows brighter amplitude contrast, confirming that its coefficient of thermal expansion is higher than that of PET. The boundary appears sharper in the micromachined probe image than in the Wollaston image. The micromachined probe also gives sharper differentiation of contrast, as shown by the wide separation between the resin and PET peaks in the corresponding data distribution (b).

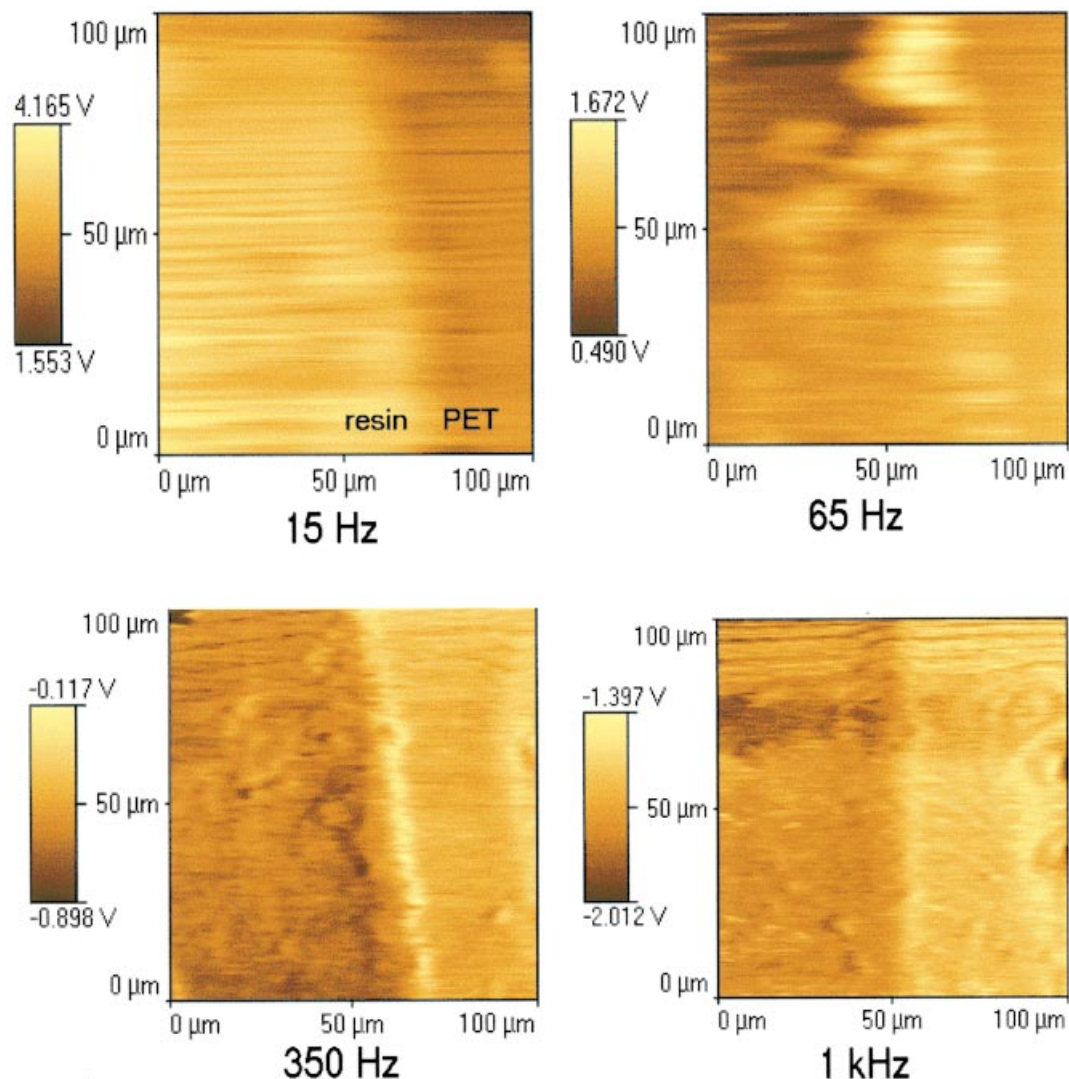


Fig. 2. SThEM: contrast reversal with increasing modulation frequency. Signal: phase images, Wollaston probe. Modulation frequencies as indicated (other details as for Fig. 1). Note the reversal in contrast between 15 and 350 Hz.

resin than for the PET, indicating a higher coefficient of thermal expansion. This is observed with both types of probe.

Clearly the ability to distinguish between two components depends on both the spatial resolution and the difference in contrast level. The figure shows that the boundary appears sharper in the micromachined probe image than in the Wollaston image. This is confirmed by the corresponding histograms of image contrast level shown in Fig. 1(b). The degree of separation between the peaks (if any) in the data distribution, corresponding to bright and dark contrast, is an indication of how well the regions are resolved as regards contrast level.

We consider first the amplitude of the thermal expansion produced at the lowest modulation frequencies (15 Hz or below). Typical amplitude values are $z_P = 2.0$ nm and

$z_r = 4.5$ nm for the PET and the resin, respectively, resulting from a Wollaston probe temperature amplitude, ΔT , of 10°C (the corresponding phase image is shown in Fig. 2a). We have measured the thermal expansion coefficients of the two materials under conditions comparable to those applying in the SThEM experiment; for this purpose it was necessary for the whole sample to be at the same temperature at any given time. For this, we used a conventional thermomechanical analyser (TA Instruments 2940 TMA) to perform modulated-temperature TMA measurements (Price, 1998). A sawtooth temperature programme consisting of repeated linear heating and cooling cycles at 1°C min^{-1} between 45 and 55°C was used, and the resulting changes in length of the samples measured. Using an average measurement of the sample thickness, the following values of the thermal expansion

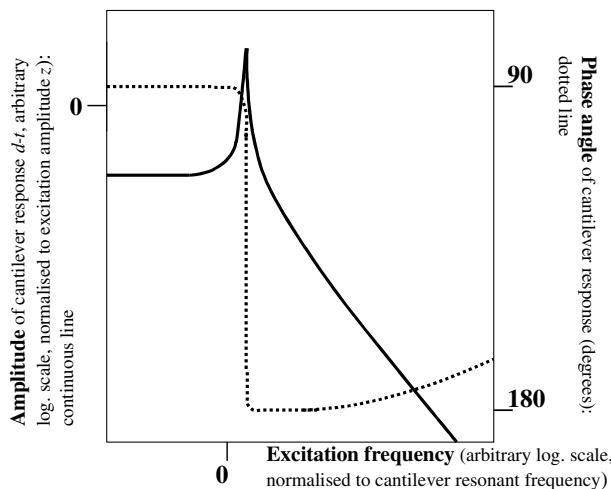


Fig. 3. Cantilever frequency response (schematic). The sample is being subjected to displacement modulation normal to its surface.

coefficients α (in units of $\mu\text{m m}^{-1} \text{K}^{-1}$) under quasi-isothermal conditions at 50°C were found to be:

PET, 63.6 ± 0.9

resin, 176.3 ± 1.2

Using the above experimental values of z_p and z_r , we divide these by the product $\alpha \Delta T$ to give a value of 2.5–3.1 μm for the effective depth of the material being heated locally during the SThEM experiment. The reason for the apparent better sensitivity of the micromachined probe at higher frequencies, and the ability of the Wollaston wire probe to differentiate between the two regions at lower frequencies, will also be largely influenced by the mechanical properties of the probe/sample system. This is discussed elsewhere (Hammiche *et al.*, 2000), where we discuss the role of two factors: (a) probe/sample contact area, and (b) volume of material heated at a given frequency as determined by the thermal diffusion length. Factor (a) favours the sensitivity of the Wollaston probe at low frequencies, whereas that of the micromachined probe is favoured at high frequencies by factor (b).

Frequency dependence

We find that at low frequencies (30 Hz or below), modulated expansion images recorded using the micromachined probe do not show any discernible contrast between the two areas. The images recorded using the Wollaston probe do show contrast between the PET and the resin, although the boundary between the two areas is not sharp. As the frequency is increased, significant amplitude contrast begins to appear at around 350 Hz in the micromachined probe images. At 700 Hz, very clear and sharp contrast is observed in the amplitude image taken with the micromachined probe, but not in the phase image. At 2 kHz and above, the contrast in the Wollaston images

decreases until at 10 kHz, sharp contrast is only observed in the amplitude image taken with the micromachined probe.

From the phase images taken with the Wollaston wire probe, we observe a reversal in contrast as the frequency is increased, as shown in Fig. 2. At 15 Hz the PET shows bright and the resin dark, indicating more phase lag when on the PET. This is reversed at 350 Hz and above, although as already mentioned, at the highest frequencies used (5 kHz and above), the contrast fades towards zero.

Effect of cantilever resonance as an explanation for the frequency dependence

The amplitude of a modulated thermal expansion signal must clearly depend on thermal conduction as well as thermal expansion, and in modelling this process it will not be easy to deconvolute the effects of the relevant properties of sample and probe. One frequency-dependent parameter is the thermal diffusion length, which for a given material, and for large probe/sample contact area, varies inversely with the square root of the modulation frequency (Almond & Patel, 1996). Accordingly, at high frequencies the volume of material heated is reduced, and we have considered whether this could explain the better sensitivity of the micromachined probe at higher frequencies, and the ability of the Wollaston wire probe to differentiate between the two regions at lower frequencies. However, a much more convincing explanation emerges if we examine a simple mechanical description of the contrast reversal effect described above.

The modulated thermal expansion of the sample/probe system will produce modulation of the vertical position of the probe–sample contact region. The effects of this will be similar to those produced when a piezoelectric actuator is used for displacement modulation of the sample height, in the well-known technique of dynamic force–distance measurement using an AFM (Burnham & Colton, 1993). In particular, the detected signal tends to a constant value at low modulation frequencies but follows a typical resonance curve as the frequency is increased. Models for interpreting the resulting measurements have recently been summarized by Burnham *et al.* (2000). When an AFM cantilever is in contact with a sample that is being subjected to displacement modulation normal to its surface (the z -direction), the amplitude and phase of the cantilever deflection, and hence the output signal, vary with frequency, as shown in Fig. 3. The functions plotted are the amplitude and phase of the normalized output signal

$$(d - t)/z = Z_s Z_E / [(Z_s + Z_h)(Z_i + Z_b)]$$

Here z is the imposed velocity of the sample position, d and t are the velocities of the base and tip of the cantilever, and the relevant mechanical impedances Z are labelled by subscripts s (force sensor, i.e. cantilever), i (interaction

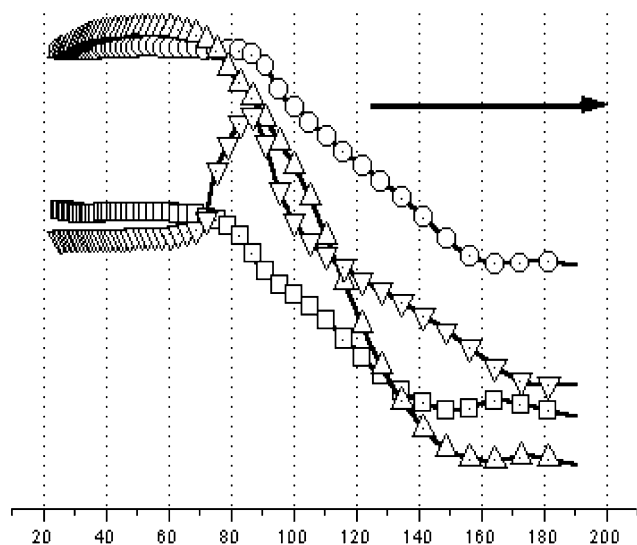


Fig. 4. Dynamic L-TMA: softening during heating. Sample: polystyrene. Indentation (onset of softening) begins at 75–85 °C, as indicated by the d.c. signals obtained as the probe temperature is increased. Here, the d.c. lateral force signal is shown. In these experiments, lateral modulation of the sample position was applied continuously but had no effect on softening temperature (different modulation frequencies are indicated by symbols as in Fig. 6).

region of the probe–sample contact), and h and b for the head and the base of the instrument. Z_E is the impedance of the entire system, defined by:

$$1/Z_E = j\omega m + 1/(Z_s + Z_h) + 1/(Z_i + Z_b)$$

Here the distributed mass of the cantilever is represented by an effective point mass m . The values of the impedances are determined by the appropriate rheological variables (Hixon, 1995), including the stiffnesses of the cantilever (force sensor) and of the sensor–sample interaction region, which we denote by k_s and k_i , respectively: we then have $Z_s = j\omega/k_s$ and $Z_i = j\omega/k_i$ if we neglect all damping terms. In the absence of attractive forces, the stiffness is related to the elasticity by the expression

$$k_i = 2E^*a$$

where E^* is the reduced elastic modulus of the tip–sample combination and a is the radius of the tip–sample contact region. In our case z is equivalent to the height of the sample surface determined by the thermal expansion, but not including the mechanical deformation produced by contact with the probe. If in addition the base and head of the instrument (cantilever mounting, sample mounting) are taken to be of infinite stiffness, the normalized output signal then approximates to

$$1/[1 + (k_s - \omega^2 m)/(k_i)].$$

Resonance such as that shown by the phase reversal and the amplitude peak shown in Fig. 3 correspond to an

infinite value of the above expression (in practice of course, damping will determine the actual peak height). For a normal AFM probe in contact with a sample of high stiffness, typical values of resonant frequency in a dynamic force–distance experiment are in the hundreds of kilohertz range. Here we find a reasonable fit to this condition using the following values for the Wollaston probe:

- $k_s = 20 \text{ Nm}^{-1}$ (measured)
- $\omega = 2\omega_c = 4\pi \times 350$ (observed frequency at which contrast reversal is seen)
- $m = 1.5 \times 10^{-6} \text{ kg}$
- $E^* = 1.5 \times 10^8 \text{ Pa}$
- $a = 30 \text{ nm}$

This set of values gives a near-maximum value for the normalized cantilever signal, according to the simplified expression above. We thus conclude that mechanical resonance is likely to be the dominant reason for the frequency-dependent contrast reversal observed. It is also likely that values of phase may be significantly affected by the rate at which the heat diffuses into the sample, and the depth of sample involved. These in turn will depend upon thermal diffusivity, and could possibly be quantified by analysis of the phase data.

Dynamic L-TMA: results and interpretation

We looked first for reliable indication of thermal events such as the glass transition temperature T_g in polystyrene. In any L-TMA experiment such as this, the signal (the vertical movement of the probe) will depend on changes in sample deformation, either elastic or plastic, under the applied load, as well as changes in thermal expansivity. In particular, abrupt increases in mechanical indentation will change the area of contact between probe and sample, and hence the applied stress and the thermal flux. Thus, it is important to observe whether a suspected thermal event, for example, occurs before or after any indentation is detected; if indentation has not yet occurred, a change in the signal could indicate some kind of precursor of indentation, rather than an independent thermal event. In principle, we might expect that any of the following could indicate that an alpha-relaxation or glass transition is occurring at a particular temperature:

- sudden onset of indentation, as detected from either the z -signal or the LFM signal
- the onset of a fall in amplitude of the modulated signal
- the endset point of the modulated or unmodulated signal, in a cooling scan (changes in probe–sample contact area less likely than during heating). By ‘endset point’, we mean the temperature at which the signal levels off to a constant value
- a peak in the phase signal.

For polystyrene we see:

1. Indentation (onset of softening) begins at 75–85 °C,

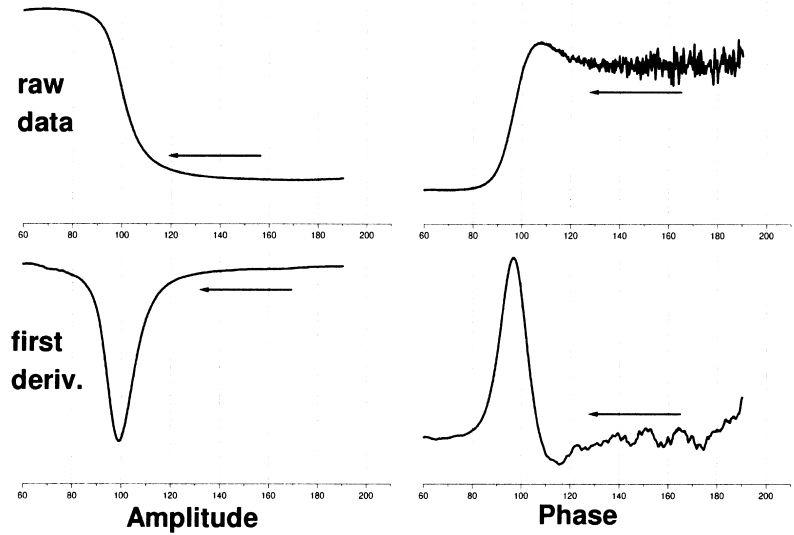


Fig. 5. Detection of glass transition of polystyrene during cooling. Signal: a.c. component of lateral force, in response to an applied 71 Hz lateral modulation of the sample position.

as indicated by the d.c. z-force data obtained during heating (Fig. 4).

2. Figure 5 shows typical a.c. data obtained during cooling, the modulation frequency being 71 Hz in this case. These data were obtained subsequent to the indentation noted above, and we assume that the detail shown indicates a genuine thermal event, whose temperature is unaffected by the indentation process. Data of this type are reproducible, and we propose that the event shown by the steep slope in the raw data indicates the glass transition.

If this is correct, T_g probably lies within the range 85–100 °C in this example. It is not at present possible to predict exactly which feature of the curve should be used to indicate a more precise value. In data from bulk TMA tests,

T_g is indicated during cooling by the ‘endset’ temperature at which the undifferentiated signal levels off to a constant value; in localized experiments we cannot assume that this will still be so, as a large temperature drop must occur within the sample over a small volume. Nevertheless, the approximate value of T_g indicated in the figure does not conflict with the bulk value for this material, for which the glass transition temperature varies as the reciprocal of molecular weight, tending to a value of $\approx 95\text{--}105$ °C at high molecular weight (Richardson & Savill, 1975).

3. Figure 6 shows the results of similar measurements performed at four different frequencies. It is interesting that a significant frequency dependence in T_g is seen. This conclusion does not depend upon which feature of the

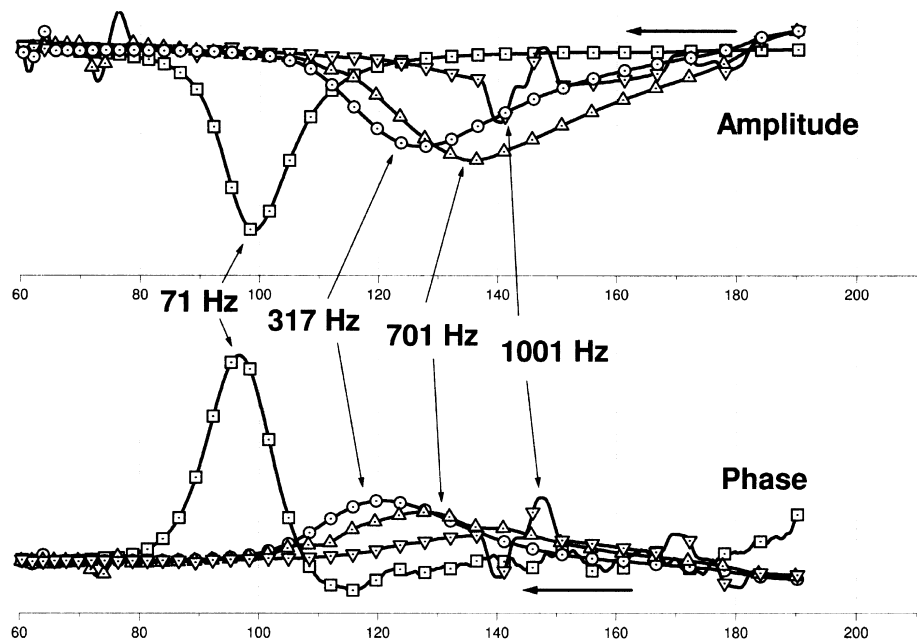


Fig. 6. T_g of polystyrene: frequency effect. Signal: as Fig. 5, but at the four different modulation frequencies shown (\square , 71 Hz; \circ , 317 Hz; \triangle , 701 Hz; ∇ , 1001 Hz). A significant frequency-dependence in T_g is seen. This conclusion does not depend upon which feature of the curves is used as the indication of T_g ; here we show the first derivative of the amplitude and phase signals.

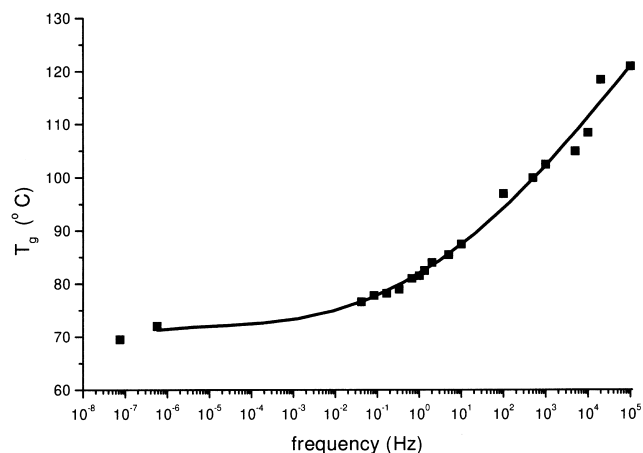


Fig. 7. T_g of bulk polystyrene (values from literature). Glass transition temperature (T_g) of bulk atactic polystyrene (Shell Carinex, molecular weight $103000 \text{ g mol}^{-1}$) vs. measurement timescale (data from Price, 1988).

curves is used as the indication of T_g : here we show the first derivative of the amplitude and phase signals. So far we have been unable to detect the β -transition which occurs at $\approx 50^\circ\text{C}$ at typical DMA frequencies (0.5–100 Hz) and is associated with local twisting of the main chain. The activation energy for this is $150\text{--}170 \text{ kJ mol}^{-1}$, and the β peak merges with the α peak at high frequencies (McCrum *et al.*, 1991). Under the conditions of our experiments (localized heating; analysis of near-surface regions), we find

that the variation with frequency is significantly greater than found for the bulk material (Fig. 7).

4. As implied earlier, we might expect that data obtained during heating could be affected by the changes in probe/sample contact geometry resulting from the indentation process. As shown in Fig. 8, during this upward temperature ramp the glass transition is not detected, and such data did indeed appear quite different from the cooling data such as we show in Fig. 5. In consequence, up/down cycles (data from both these figures, for example) showed marked hysteresis. It is interesting that the same effect was found in the unpublished experiments performed previously using z -modulation (for an example of data, see Fig. 11 of Reading *et al.*, 1998). This was in spite of the fact that when z - rather than x -modulation is used, the danger of probe/sample sliding is greater, as discussed above, especially at the large modulation amplitudes used in the z -modulation experiments (up to $1 \mu\text{m}$).

The positions of the peaks in the heating experiments are too high to indicate T_g . The hysteresis suggests that here, the relaxation does not occur until the indentation has been completed; one possibility is that the moving probe orients the polymer in some way, so that a region of rigidified material is formed around the probe tip, and the glass transition is thereby inhibited. Also, the increased contact area produced by indentation could produce a marked increase in thermal expansion. On cooling, this indentation effect is absent, so that T_g occurs as noted above.

Future experiments will include a study of cross-linked polystyrene, and tests in which the heating is repeated after

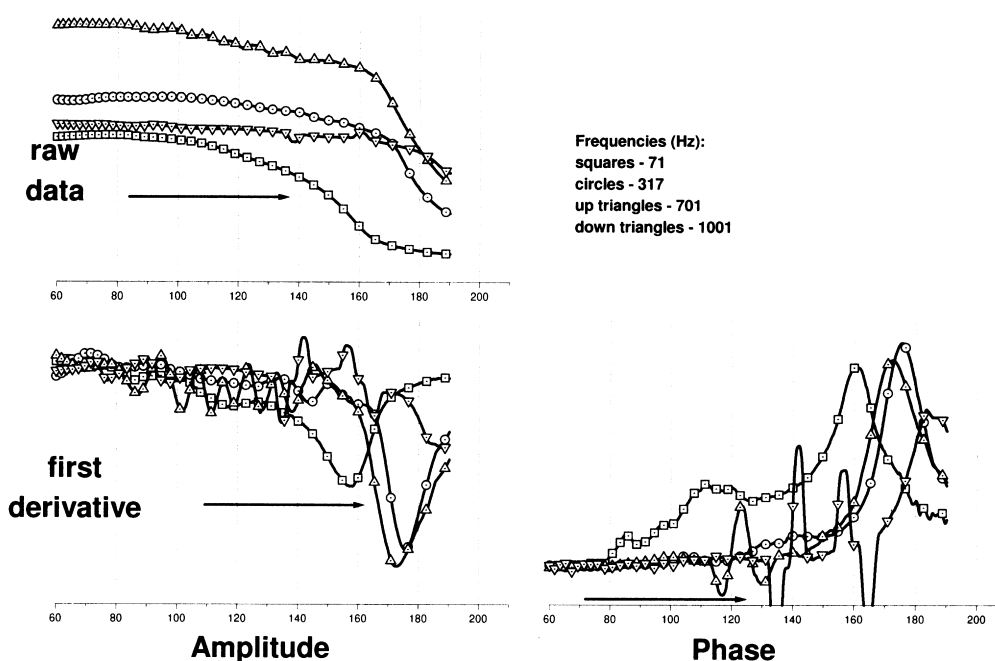


Fig. 8. a.c. signals: complications resulting from the indentation process during heating. Signal: as Fig. 5, but for increasing localized temperature. Modulation frequencies as shown in Fig. 6. The glass transition is not detected. The features of these curves differ from those shown by the cooling data (Fig. 5) and by the d.c. data (Fig. 4).

a heat/cool cycle. In Price *et al.* (1999) we comment on possible alternative configurations for dynamic L-TMA. For example, the application of the force could be determined by modulation of the cantilever position. Alternatively, the position of the tip itself could be modulated either magnetically or by means of thermal expansion of the tip, when a modulated temperature programme is applied to it. Further work is needed to explore the possible value of different imaging modes; in some preliminary experiments, we have found it possible to obtain images whose contrast is determined by the magnitude of the a.c. amplitude or phase signal.

Conclusions

Scanning thermal expansion microscopy has been shown to give useful image contrast over a frequency range of 15–2000 Hz. A reversal in contrast is seen under certain conditions as the frequency is increased, and is explained in terms of mechanical resonance of the cantilever. For polymer/resin samples, the depth of material contributing to the measured thermal expansion is typically a few micrometres. It is possible that the method could be developed to provide quantitative mapping of spatial variation in thermal expansivity. It would be necessary to deconvolute the role of thermal conductivity (using data from unmodulated thermal images) and diffusivity (which, together with modulation frequency, determines the depth of penetration of the thermal wave). The contribution of the probe would be calibrated using a reference material of known thermal properties.

In experiments on dynamic localized thermomechanical analysis, we have detected the glass transition of polystyrene, which shows a significant variation with frequency. In conventional bulk DMA, materials are characterized through changes in the real and imaginary parts of the elastic modulus. With this 'localised' version of DMA, it will be possible to profit from the chief advantages of using the active thermal probe to provide the temperature change as well as the modulation, without the use of a heating stage, namely: (a) the data are obtained from localized regions chosen from a previously obtained thermal image, (b) apart from these regions, the rest of the sample is preserved in its original unheated state.

For many materials, thermal transitions have a greater effect upon thermal expansion coefficient and elastic modulus than upon thermal conductivity or heat capacity. Accordingly, these localized versions of thermomechanical modulation may well prove useful in the detection of thermal events.

Acknowledgements

We thank N. A. Burnham, M. Conroy, D. J. Houston and M. Song for valuable advice and discussion. Part of the

research was carried out during the tenure by one of us (H.M.P.) of a visiting professorship at EPFL. This work was made possible by funding from the Engineering and Physical Sciences Research Council.

References

- Almond, D.P. & Patel, P.M. (1996) *Photothermal Science and Techniques*. Chapman & Hall, London.
- Burnham, N.A., Baker, S.P. & Pollock, H.M. (2000) A model for mechanical properties nanoprobe. *J. Mater. Res.* in press.
- Burnham, N.A. & Colton, R.J. (1993) Force microscopy. *Scanning Tunnelling Microscopy and Spectroscopy: Theory, Techniques and Applications* (ed. by D. A. Bonnelli), pp. 191–249. VCH Publishers, New York
- Fryer, D.S., dePablo, J.J. & Nealey, P.F. (1998) Investigation of photoresist and the photoresist/wafer interface with a local thermal probe. *Proc. SPIE*, **3333**, 1031–1039.
- Hammiche, A., Bozec, L., Conroy, M., Pollock, H.M., Mills, G., Weaver, J.M.R., Price, D.M., Reading, M., Hourston, D.J. & Song, M. (2000) Highly localised thermal, mechanical and spectroscopic characterisation using miniaturised thermal probes. *J. Vac. Sci. Technol. B*, **18**(3), 1322–1332.
- Hammiche, A., Pollock, H.M., Hourston, D.J. & Reading, M. & Song, M. (1996b) Scanning thermal microscopy: sub-surface imaging, thermal mapping of polymer blends, localised calorimetry. *J. Vac. Sci. Technol.* **B14**, 1486–1491.
- Hammiche, A., Reading, M., Pollock, H.M., Song, M. & Hourston, D.J. (1996a) Localised thermal analysis using a miniaturised resistive probe. *Rev. Sci. Instrum.* **67**, 4268–4274.
- Hixon, E.L. (1996) Mechanical impedance. *Shock and Vibration Handbook* (ed. by C. M. Harris), pp. 10.1–10.10. McGraw-Hill, New York.
- Mazeran, P.-E. & Loubet, J.-L. (1997) Force modulation with a scanning force microscope: an analysis. *Tribology Lett.* **3**, 125–132.
- McCrum, N.G., Read, B.E. & Williams, G. (1991) *Anelastic and Dielectric Effects in Polymeric Solids*. Dover, New York, pp. 409–415.
- Oulevey, E., Burnham, N.A., Gremaud, G., Kulik, A.J., Pollock, H.M., Hammiche, A., Reading, M., Song, M. & Hourston, D.J. (2000) Dynamic mechanical analysis at the submicron scale. *Polymer*, **41** (8), 3087–3092.
- Oulevey, E., Gremaud, G., Semoroz, A., Kulik, A.J., Burnham, N.A., Dupa, E. & Gourdon, D. (1998) Local mechanical spectroscopy with nanometer-scale lateral resolution. *Rev. Sci. Instrum.* **69**, 2085–2094.
- Pollock, H.M., Hammiche, A., Song, M., Hourston, D.J. & Reading, M. (1998) Interfaces in polymeric systems as studied by CASM – a new combination of Calorimetric Analysis with Scanning Microscopy. *J. Adhesion*, **67**, 217–234.
- Price, D.M. (1988) *Synthesis and characterisation of polyester-ester block copolymers*. PhD Thesis, University of Birmingham.
- Price, D.M. (1998) Novel methods of modulated-temperature thermal analysis. *Thermochimica Acta*, **315**, 11–18.
- Price, D.M., Reading, M., Caswell, A., Hammiche, A. & Pollock, H.M. (1998) Micro-thermal analysis: a new form of analytical microscopy. *Eur. Microsc. Anal.* **65**, 17–19.
- Price, D.M., Reading, M., Hammiche, A. & Pollock, H.M. (1999)

- Micro-thermal analysis: scanning thermal microscopy and localised thermal analysis. *Int. J. Pharmaceut.* **192**, 85–96.
- Reading, M. & Haines, P.J. (1995) Thermomechanical, dynamic mechanical and associated methods. *Thermal Methods of Analysis: Principles, Applications and Problems* (ed. by P. J. Haines), pp. 123–160. Blackie, London.
- Reading, M., Hourston, D.J., Song, M., Pollock, H.M. & Hammiche, A. (1998) Thermal analysis for the 21st century: μ TA. *Am. Lab.* **30** (1), 13–17.
- Richardson, M.J. & Savill, N.G. (1975) Derivation of accurate glass transition temperatures by differential scanning calorimetry. *Polymer*, **16**, 753–757.
- Varesi, J. & Majumdar, A. (1998) Scanning Joule expansion microscopy at nanometer scales. *Appl. Phys. Lett.* **72** (1), 37–39.
- Zhou, H., Midha, A., Mills, G., Thoms, S., Murad, S.K. & Weaver, J.M.R. (1998) Generic scanned-probe microscope sensing by combining micromachining and electron beam lithography. *J. Vac. Sci. Technol.* **B16**, 54–58.